Modeling the Nucleation Stage during Batch Emulsion Polymerization

Montserrat Fortuny, Christian Graillat, and Timothy F. McKenna
Laboratory for the Chemistry and Processes of Polymerization (LCPP–CNRS), Ecole Supérieure de Chimie, Physique et Electronique de Lyon (ESCPE), 69616 Villeurbanne Cedex, France

Pedro H. H. Araújo
Chemical Engineering Program (EQA), CTC, Federal University of Santa Catarina (UFSC), Florianópolis, Brazil

José C. Pinto
Programa de Engenharia Quimica/COPPE, Universidade Federal do Rio de Janeiro, Rio de Janeiro-21945-970, RJ Brazil

DOI 10.1002/aic.10516
Published online June 22, 2005 in Wiley InterScience (www.interscience.wiley.com).

A model based on independently validated stabilization and rate data is used to quantify the rate of formation of particles during the dynamic nucleation stage of a batch emulsion polymerization reaction. Population balance equations (PBEs) that combine kinetic data validated in the absence of coagulation and a DLVO stability model with parameters validated in the absence of reaction were used to account for both micellar and homogeneous nucleation, as well as particle stabilization and growth. The model was tested in different polymerization systems at different ionic strengths. It is shown that a large number of moderately short-lived particles are formed during the early stages of nucleation and that they contribute to an accelerated rate of polymerization for a short period of time before coagulating onto large structures in the reactor. © 2005 American Institute of Chemical Engineers *AIChE J,* 51: 2521–2533, 2005
Keywords: particle size distribution (PSD), emulsion polymerization, nucleation, electrosteric surfactant, modeling

Introduction

Particle nucleation is perhaps the most controversial aspect of emulsion polymerization reactions. The formation of the initial particles occurs very quickly, and different mechanisms must be simultaneously taken into account.[1-3] The experimental study of the nucleation stage is a difficult task because of the complexity and rapidity of the phenomena involved, as well as technical limits on the measurement of particle size distributions (PSDs) and the in-line/real-time monitoring of particle formation. Recent studies based on the development of conductivity sensors for the on-line monitoring of surfactant concentrations during emulsion polymerizations[4] indicate that conductivity data can provide useful information about the particle nucleation stage and provide direct quantitative evidence of what has long been postulated theoretically (such as coagulative nucleation theory[5]): the profile of particle generation (that is, the evolution of the number of particles as a function of time) is not monotonically increasing, and that a large number of primary particles are formed in a short period of time and these particles coagulate to form the basis of the final particle population.

Of course numerous experimental and theoretical studies have also been presented in the literature to improve the understanding of mechanisms that may influence particle nucleation[3,6-8] and coagulation.[9-13] In the earliest works on particle nucleation, the studies are based on assumptions that are not completely true. For instance, three of the most common ideas

Present address of M. Fortuny: Instituto de Tecnologia e Pesquisa (ITP), Universidade Tiradentes (UNIT), Aracaju, Brazil.
Correspondence concerning this article should be addressed to T. F. McKenna at mckenna@cpe.fr.

were that (1) particle nucleation terminates at the end of interval I if the monomers are not particularly water soluble (that is, when micelles are no longer present in the system), (2) the final number of polymer particles can be obtained at the end of this interval, and (3) the polymer particles formed through the micellar mechanism are colloidally stable.[6-8] It is now widely accepted that different mechanisms may take place simultaneously during the nucleation stage and that experimental conditions can modify the influence of each particular phenomenon on the particle nucleation. These include micellar nucleation,[14-16] homogeneous nucleation,[17-19] coagulative nucleation,[5] and emulsified monomer droplet nucleation[20-22] (although the latter mechanism is often assumed to be negligible). Although significant progress has been made in understanding the mechanisms of particle creation and stabilization, much work remains to be done in terms of generating robust mathematical descriptions of emulsion polymerizations ab initio.

Useful mathematical models, based on sophisticated techniques such as population balance equations (PBEs), have been developed and implemented to describe the nucleation stage in batch processes, as well as to combine different aspects of particle growth (that is, kinetics) with models of particle stabilization and nucleation to predict the entire PSD in emulsion polymerizations.[23-29] The nucleation models and kinetic mechanisms are coupled to describe the evolution of conversion and diameter of polymer particles (*Dp*) [or number of polymer particles (*Np*)] experimental data. These models require the knowledge of a set of kinetic parameters, and parameters allowing us to calculate the coagulation coefficients that are typically obtained by fitting experimental conversion and *Np* data, usually acquired by analysis of samples off-line. However, it is our opinion that model fits based on *Np* data taken during periods of rapid particle formation must be treated with caution for at least two reasons: (1) because the available experimental techniques are still unable to provide reliable measurements of particle diameters for very small particles formed in the early stages of the reaction[30,31]; (2) it is more than possible that the simple act of extracting samples from the reactor and diluting them to perform particle size measurements can alter the stability of the particles (especially the smaller ones). An extensive review of the literature on PBE modeling (including a number of articles not cited above) leads us to conclude that no previous modeling studies have included all of these phenomena using independently validated data, and there are no published reports that allow us to quantify the extent to which the dynamics of particle nucleation and coagulation influence *Np* in a rapidly changing system.

As mentioned above, conductivity studies suggest that a large fraction of the particles created at the very beginning of the nucleation stage are only "meta-stable," in other words they exist for short periods of a few minutes, but cannot be stabilized for a number of reasons, and thus disappear rapidly. In this case, these particles can contribute to the polymerization reaction and the consumption of monomer, but will not be detected by off-line measurement techniques, especially quasi-elastic light scattering because, by the time the measurements are made, these particles are no longer present (the dilution of the samples required to perform these measurements does not help either).

A general mathematical framework and approach based on PBEs is therefore proposed in this work to circumvent some of the difficulties enumerated earlier, thereby providing a means of quantifying the number of particles present in an ab initio batch emulsion polymerization. The main objective here is to use a well-constructed mathematical model, based on known theories of particle formation, stabilization, and kinetics to quantify the rate of formation of particles during the dynamic nucleation stage of an emulsion polymerization reaction. The originality of the approach lies in the combination of independently validated "submodels" based on DLVO (Derjaguin–Landau–Verwey–Overbeek) theory, and a kinetic model for the polymerization of butyl acrylate in a manner that ensures that physical phenomena are accurately described. The particle coagulation part of the model has only one adjustable parameter (the Hamaker constant) that is measured in a nonreacting system to avoid simply adjusting the stability parameter to fit experimental data in reacting systems.[32,33] Monomer partitioning,[34] among the many phases of the reaction system, was measured in inert systems, and particle growth kinetics were validated in the absence of coagulation in a seeded reactor. This means that, because each particular phenomenon was studied independently (both theoretically and experimentally), there should be no correlation between the model parameters—in other words this approach means that we avoid the pitfall of fitting both stability and kinetic parameters from one set of experiments. This in turn allows us to quantify with confidence the evolution of the number of particles during the dynamic nucleation stage. The model is then tested on butyl acrylate and methyl methacrylate emulsion copolymerizations using an anionic surfactant, with different ionic strengths in the medium.

Experimental

Batch emulsion copolymerizations were performed with a monomer composition of 80% butyl acrylate (BuA) and 20% methyl methacrylate (MMA) by weight. Both monomers were stabilized with hydroquinone. Ammonium persulfate (APS) was used as initiator. These reagents were obtained from Acros Organics (Geel, Belgium) and used as received. The anionic electrosteric surfactant Disponil® FES 32 IS (sodium salt of the sulfate of a polyglycol ether, abbreviated here as "TA") and the nonionic Disponil® A3065 (mixture of linear ethoxylated fatty acids, abbreviated here as "TN") were used to stabilize polymer particles. The surfactants were supplied by Cognis (Meaux, France) and used as received.

Latices were prepared in a 3-L jacketed glass vessel connected to a condenser to avoid the loss of monomers through evaporation. The reactor temperature was rightly controlled through manipulations of the flow of cool water added into the cooling bath. First, the chemical components, with the exception of the initiator, were fed into the reactor. The mixture was then purged with hydrogen for 30 min to remove residual oxygen. The mixture was heated up to the reaction temperature equilibrium at 70°C under continuous stirring conditions. After this, initiator solution was added into the reactor to start the polymerization. Samples were collected at regular intervals and monomer conversion and average particle diameter (*Dp*) were measured. Monomer conversion was determined by gravimetry and *Dp* was measured using a Malvern LoC and Malvern

Multiangle apparatus (Autosizer 4800), both based on a quasi-elastic light-scattering technique.

Mathematical Model

A mathematical model was developed for batch emulsion copolymerizations stabilized by anionic surfactants. The main objective was the description of the evolution of monomer conversion coupled with that of the PSD, and to validate the model without using parameters fitted from the dynamic experiments. In principle, these variables can be represented through a PBE if the several physicochemical phenomena occurring in an emulsion polymerization are taken into consideration. The following sections cover each of these important phenomenological aspects that occur during emulsion polymerization reactions. The model was built based on the following set of assumptions:

- The reactor is perfectly mixed.
- Radical balances in the aqueous phase are solved at stationary conditions.
- Monomer concentrations in the different phases are at thermodynamic equilibrium.
- Kinetic constants are considered to be the same for both aqueous and polymer phases.
- Radicals formed by initiator decomposition and by transfer reactions have similar kinetic behavior.
- Particles are formed through both micellar and homogeneous nucleation.
- Compartmentalization of radicals into polymer particles can be neglected (pseudo-bulk kinetics).

Kinetics

The kinetic mechanism used in the proposed model includes the polymerization rates in both aqueous and particle phases. The aqueous phase mechanism involves initiator decomposition, which forms radicals that can propagate, terminate, or enter into polymer particles. Radical entry may occur if the degree of radical size is above a critical value for entry (z). Radicals of size greater than the critical degree of solubility (j_{crit}) precipitate and form a new particle. When radicals enter into polymer particles, they can propagate, terminate, or desorb from the particle (if the radical activity is transferred to a monomer unit).

Based on this standard kinetic mechanism, mass balances for radical species in the aqueous phase were described and solved for the steady-state conditions. The radical balances will not be shown here for the sake of brevity (see Appendix) and the detailed approach can be found in Fortuny[32] and Araújo et al.[35,36] For polymer particles, the kinetic model influences the computation of the average number of radicals per particle ($\bar{n}$). As reported by Unzueta and Forcada,[23] the pseudo-bulk approximation can be used for BuA–MMA emulsion copolymerizations, and $\bar{n}$ may be computed using the equation developed by Ugelstad et al.[37]

Monomer partitioning

Monomer partitioning can have a significant influence on phenomena occurring in the aqueous phase. For relatively highly water soluble monomers such as MMA, the precise modeling of the polymerization reactions requires the accurate description of monomer partitioning. Thermodynamic and semiempirical approaches described in the literature were reviewed by Fortuny et al.[34] and compared to experimental data obtained from film partitioning measurements. The authors presented a complete study of the partitioning of mixtures of MMA and BuA in BuA–MMA copolymers. The experimental data for this system were successfully fitted through the semiempirical model proposed by Maxwell et al.[38,39] Based on this work, the Maxwell approach was used to describe monomer partitioning. The details about this model can be found in Fortuny et al.[34] and the Appendix at the end of the text.

Nucleation

The mathematical representation of the nucleation step was based on the competition of both micellar and homogeneous nucleation mechanisms. For micellar mechanism, the nucleation rate was computed as a function of the micelle concentration (N_{mic}) as follows:

$$NucMi = k_{mic} N_{mic} [R_{ent}]_{aq} \tag{1}$$

where the term $[R_{ent}]_{aq}$ is the concentration of oligoradicals in the aqueous phase that can enter into particles and k_{mic} is the rate constant for oligoradical absorption into micelles.

For the homogeneous mechanism, the nucleation rate is related to the rate of formation of radicals with size j_{crit}. The homogeneous nucleation rate is then expressed as

$$NucHo = N_A V_{aq} k_p [M]_{aq} [R_{j_{crit}-1}]_{aq} \tag{2}$$

where N_A is the Avogadro number, V_{aq} is the volume of the aqueous phase, k_p is the propagation rate constant, $[M]_{aq}$ is the monomer concentration in the aqueous phase, and $[R_{j_{crit}-1}]_{aq}$ is the radical concentration of size $j_{crit} - 1$.

The relative importance of each nucleation mechanism is influenced by the experimental conditions. According to standard nucleation models, when the surfactant concentration is above the critical micellar concentration (CMC), micelles are formed and micellar nucleation is the dominant mechanism. Oligoradicals formed in the aqueous phase with size between z and $j_{crit} - 1$ may enter into the swollen-monomer micelles and generate the first polymer particles. The micelle diameter is of the order of a few nanometers and the corresponding overall interfacial area is high enough to absorb a great number of oligoradicals, thus reducing the amount of available radicals in the aqueous phase that would propagate and form particles through the homogeneous mechanism. The standard nucleation model predicts that the homogeneous mechanism may become important when polymer particles are nucleated and absorb surfactant molecules from the reaction media to become colloidally stable, reducing the micelle concentration, in the system and consequently the rate of micellar nucleation. The contribution of the homogeneous mechanism may depend on several factors such as the surfactant concentration, the kinetics of the radicals in the aqueous and particle phases, and the monomer hydrophilic characteristics. All these aspects were taken into account to model the partitioning of the surfactant and monomer species, among the many phases inside the reactor.[34]

Both micellar and homogeneous mechanisms result in the nucleation of tiny particles a few nanometers in diameter. As predicted by classical theories of the electrostatic stability,[40-42] the stability of very small colloidal species can be guaranteed only when the surface charge densities are large. These conditions can be attained only when the number of polymer particles is small. When a high number of polymer particles are nucleated, the amount of available surfactant for particle stabilization can be insufficient to avoid the coagulation of the tiny particles. Then, the number of polymer particles must be related to both nucleation and coagulation phenomena. Therefore, the appropriate modeling of nucleation and coagulation is required to obtain an accurate description of the PSD.

Coagulation

In an earlier study,[32,33] the stability and, in particular, the values of the Hamaker constant for different species (sulfate groups and TA) were studied for the case of BuA–MMA copolymerization. Stability data were obtained based on turbidity measurements. In these studies, coagulation between the particles *in the absence of reaction* was provoked by electrolyte addition. The experimental stability data and an electrostatic stability model based on the DLVO theory[40,41] were used to estimate the Hamaker constants for the TA system. The electrostatic stability model was incorporated into the population balances for nonreacting systems and was successfully validated for coagulation experiments[33] in which polymer particles were destabilized by electrolyte addition. Based on these results, the model in question can be used for the theoretical description of the coagulation between particles in the reacting systems with confidence. The coagulation rate between two polymer particles was calculated as a function of the ratio (r) of each polymer particle as described by the following equation:

$$B_{ij} = B_{ji} = \frac{2k_B T}{3\eta W_{ij}} \frac{(r_i + r_j)^2}{r_i r_j} \tag{3}$$

where k_B is the Boltzmann constant, T is the medium temperature, η is the latex viscosity, and W_{ij} is Fuch's stability ratio.

Population balances

The PBE includes the most important phenomena that can influence the evolution of the number of individual particles, such as nucleation, coagulation, and growth of polymer particles. The number density of the PSD was denoted as $N(m_i, t)$, where the polymer mass (m) was taken as the characteristic dimension of the polymer particles. The general form of the PBE was derived by Araújo et al.[36] and adapted in this work for batch processes as described by the following equation:

$$Np\frac{\partial f(m_i,t)}{\partial t} + f(m_i,t)\frac{\partial Np}{\partial t} + Np\frac{\partial[cr(m_i)f(m_i,t)]}{\partial m_i} = -\frac{f(m_i,t)}{V_R}N_p^2\int_{m_0}^{m_f}\beta(m_i,m_j)f(m_i,t)dm_j + \frac{N_P^2}{2V_R}\int_{m_0}^{m_i-m_0}\beta(m_i-m_j,m_j)f(m_i-m_j,t)f(m_i,t)dm_j + NucMi(m_i) + NucHo(m_i) \tag{4}$$

where Np is the total number of polymer particles, $f(m_i, t)$ is the number fraction density of the PSD, V_R is the reaction volume, $\beta(m_i, m_j)$ is the coagulation rate between two polymer particles of mass m_i and m_j, and $cr(m_i)$ is the mass growth rate of polymer particles arising from the polymerization reaction.

The first two terms on the left-hand side of this equation describe the time rate of change of the number of polymer particles of mass m_i, whereas the third term represents the mass change of the number density function arising from the polymerization reaction. The terms on the right-hand side of the PBE take into account the rates of formation of particles of mass $m_i + dm_i$ resulting from the coagulation of particles of mass m_i, the rate of formation of particles of mass m_i stemming from the coagulation of smaller polymer particles, and the nucleation rates of particles of mass m_i through the micellar and homogeneous mechanisms, respectively.

Therefore, the overall balance of polymer particles can be written as

$$\frac{\partial Np}{\partial t} = -\frac{1}{4}N_p^2\int_{m_0}^{m_f}\int_{m_0}^{m_f}\beta(m_i,m_j)f(m_j,t)f(m_i,t)dm_j dm_i + NucMi + NucHo \tag{5}$$

The PBE can be solved after introduction of the coagulation and nucleation rate expressions, of the differential mass balance equations for all chemical species (initiator, monomers, surfactant, and polymer), definition of the reaction volume, and the determination of the kinetic parameter $\bar{n}$, as proposed by Ugelstad et al.,[37] based on the pseudo-bulk approach. To solve the PBE, the entering domain of mass polymer particles is discretized into 200 mesh points using regular central finite differences. Numerical integrations were performed with the help of the DASSL procedures.[43]

It is important to point out here that what is important in this approach is that the different terms in the PBE are validated separately to eliminate correlation between the terms insofar as possible. In other words, the kinetic model is validated (see below) in the absence of nucleation and coagulation, and the model for coagulation (and the relevant parameters) was validated in the absence of reaction. This allows us to use the mathematical tool to infer more detailed information about the process of nucleation than would be possible if we simply fit the parameters needed for Eq. 5 to off-line data obtained during a batch polymerization run.

Results and Discussion

Kinetic model validation

The description of the kinetic mechanism of this copolymerization system includes a large set of kinetic parameters (see Tables 2 and 3 below). The validation of the kinetic model for batch emulsion polymerization is a difficult task because nucleation, coagulation, and polymerization can take place simul-

Table 1. Recipes for Seeded Semibatch Reactions

	CA1	CA2	CA3	CA4	CA5
			Characteristics of the Seed Particles		
Dp, nm	149	155	254	265	140
Np	3.6×10^{16}	3.2×10^{16}	2.8×10^{16}	1.2×10^{16}	4.3×10^{16}
			Preemulsion Recipes		
Duration, min	88	72	68	298	478
Feed rate, g min^{-1}	3.1	7.8	7.6	1.7	1.1
Water, g	81	169	154	100	239
TA, g	5.8	12.1	11.0	12.3	4.8
BuA, g	146	306	278	434	177
MMA, g	37	77	70	109	44
APS, g	0	0	0	0.46	0.22

taneously. To isolate the "kinetics" from coagulation and nucleation-related phenomena, the model was validated for seeded semibatch reactions under well-controlled conditions of stabilization to avoid secondary nucleation (insofar as this is possible) and coagulation between polymer particles. For this reason, only a nonionic surfactant TN was added during the semibatch step at a rate that ensured that the particle surface coverage was always $<100\%$ (N.B.: surface coverage refers to the percentage of the particle surface covered by the surfactants). The semibatch step was conducted with addition of water, monomers, surfactant, and initiator (only for long reactions). All these components were previously emulsified and added into the reactor through a single feed stream. The feed flow rate was deliberately modified from run to run to maintain starved or nonstarved conditions. The temperature was kept constant at 70°C during the reaction. Table 1 shows recipes and experimental conditions for the semibatch reactions, used to validate the kinetic model.

Figure 1 shows model simulations and experimental data for the evolution of the monomer conversion and *Dp* as a function of time. The values of the kinetic constants used in the simulations are listed in Tables 2 and 3. Note that all the kinetic parameters were obtained from the literature, with the exception of the gel effect parameters (a_1 and b_1) that were estimated from available experimental conversion data. The set of kinetic parameters allows for a satisfactory prediction of monomer conversion and particle diameter for all five experiments. Note that the experimental conversion for the semibatch step was varied in a large range of 0.55 to 0.92, showing that the kinetic model is appropriate for starved and nonstarved semibatch reactions. Thus the proposed kinetic model is well suited to provide good description of a range of conditions, including batch processes.

PBE validation for batch processes

As mentioned earlier, mathematical models were developed to describe the main phenomena involved in batch emulsion polymerization processes and were validated for simplified experimental systems. Coagulation between polymer particles was studied for nonreacting systems, partitioning of monomers between polymer and aqueous phases was compared successfully to partitioning measurements, and the kinetics of the copolymerization was validated for seeded semibatch reactions. This information was then coupled with the nucleation models (Eqs. 1 and 2) and included in the PBE (Eq. 3). The nucleation model requires the knowledge of several model parameters for the anionic surfactant system, such as the specific surfactant area (a_s), the critical micellar concentration (*CMC*), the micelle radius, and the efficiency of the radical entry into the micelles (f_{mic}). Table 3 presents the parameter values used to perform the simulations of the batch processes. Most of the parameters were measured or taken from values reported in the literature. The only fitted parameter was f_{mic}, which can not be obtained through independent experiments. This parameter was estimated by sensitivity analysis, performed through the optimization of the quadratic differences between observed and predicted conversion data.

The use of conversion data for parameter fitting is justified in this case by the fact that the available experimental techniques for conversion measurement are more reliable than those used to determine *Dp* (or *Np*). These techniques are generally based on light-scattering devices that provide uncertain values for too small particles and large PSD, usually formed during the earliest stages of the polymerization. Figure 2 shows experimental and simulated data of monomer conversion, *Np* and *Dp*, respectively, for a batch polymerization run performed with an anionic surfactant concentration of $2 \times CMC$. Note that the model gives a reasonable description of the experimental conversion (Figure 2A), as expected, once the adjustable parameter f_{mic} was fitted through the optimization of conversion curves. On the other hand, the evolution of *Np* as predicted by the model is quite different from the experimental values obtained in the early stages of the reaction (Figure 2B). In fact, the model predicts that during the early stages of nucleation, a large number of moderately short-lived particles are formed, contributing to an accelerated rate of polymerization for a short time. As *Np* increases, the amount of available surfactant molecules for particle stabilization decreases up to a limit value from which particles start coagulating onto large structures inside the reactor. At the end of the polymerization run, there is a good agreement between the predicted and the observed *Np* values. At this time, the diameters of polymer particles are sufficiently large to be detected precisely through light-scattering measuring techniques.

The resulting *Np* profile provided by the model is completely different from those generally found in the literature concerning monomers with relatively high water solubility.[25,29] To investigate whether this profile might indeed be feasible, the evolution of monomer conversion during the batch polymerization was simulated assuming that the dynamic *Np* profile

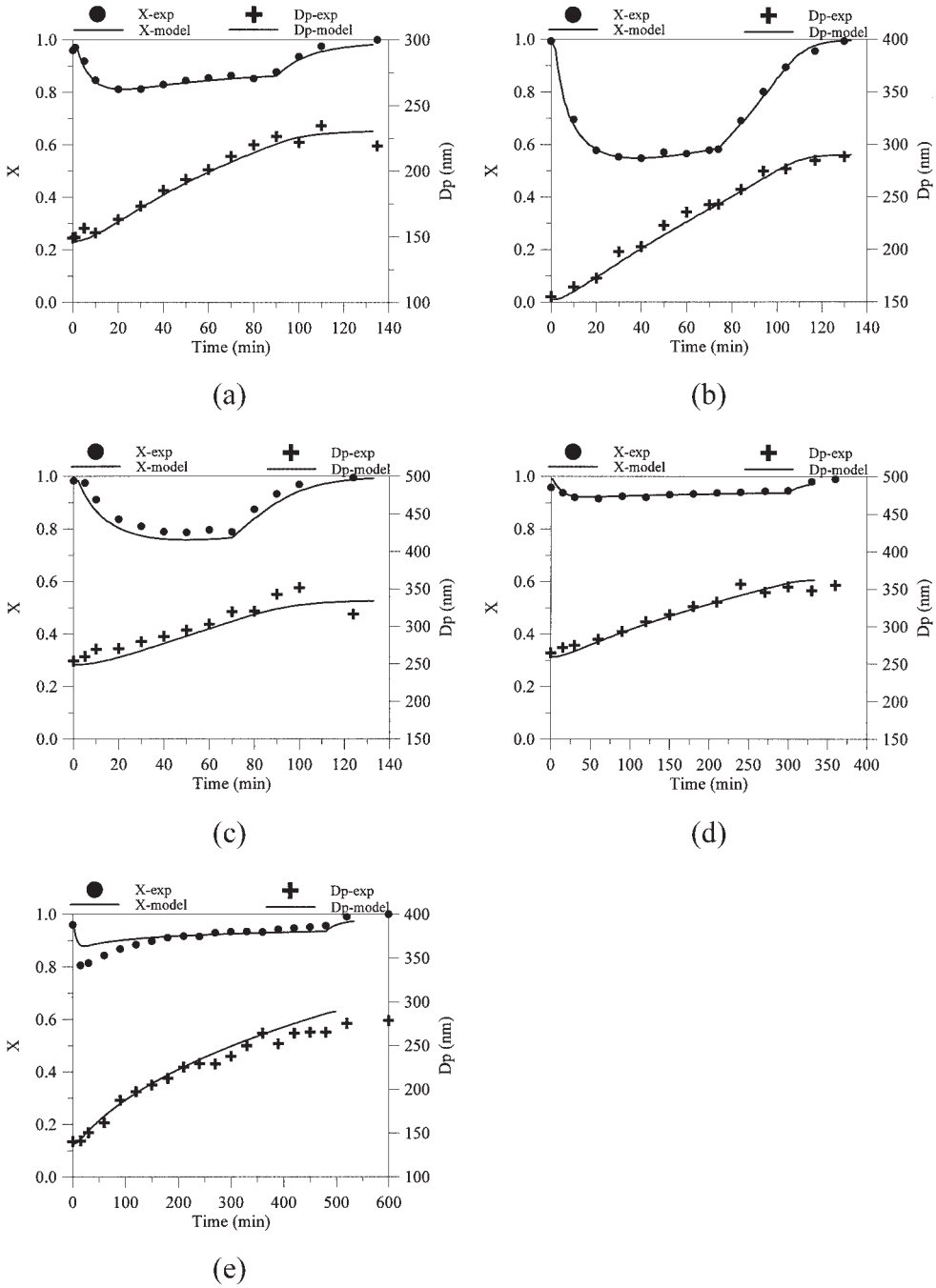

Figure 1. (A) Evolution of monomer conversion and *Dp* for seeded semibatch CA1. (B) Evolution of monomer conversion and *Dp* for seeded semibatch CA2. (C) Evolution of monomer conversion and *Dp* for seeded semibatch CA3. (D) Evolution of monomer conversion and *Dp* for seeded semibatch CA4. (E) Evolution of monomer conversion and *Dp* for seeded semibatch CA5.

(profile 1) was similar to the experimental one (that is, rather than calculating *Np* the values measured off-line were used to calculate the conversion). In these simulations the PBE was replaced by an empirical equation used to interpolate the experimental *Np* data as a function of time, so that the *Np* profile was not determined from nucleation models. These *Np* values were fed into the kinetic model to simulate the evolution of monomer conversion. Figure 3 shows results for the batch run described previously. The results clearly show that the monomer conversion is underestimated if the "experimental" profile of *Np* is assumed to be correct (profile 1). On the other hand, different *Np* profiles were tested varying parameter f_{mic} to match experimental conversion data and kinetic model results. The best attempt was given by profile 2, shown in Figure 3. Not surprisingly, the shape of the *Np* curve is very similar to the output of the nucleation models included in the PBE, which strongly suggests that the simulated *Np* profile could be very close to the actual evolution of the number of polymer particles

Table 2. Parameter Values Used in the Kinetic Model

Parameter	Value	Reference
a_1	-4.03	Estimated
b_1	-0.66	Estimated
D_{aq} (dm^2 s^{-1})	0.1	46
j_{crit}	10	1
k_{mic}	$4\pi D_{aq} r_{mic} N_A f_{mic}$	25
k_p (BuA) (dm^3 mol^{-1} s^{-1})	$7.40 \times 10^7 \exp\left(-\frac{9600}{8.3144T}\right)$	47
$k_{p\text{BuA–MMA}}$	$k_p(\text{BuA})/r_{\text{BuA–MMA}}$	48
$k_{p\text{MMA–BuA}}$	$k_p(\text{MMA})/r_{\text{MMA–BuA}}$	48
k_p(MMA) (dm^3 mol^{-1} s^{-1})	$2.66 \times 10^7 \exp\left(-\frac{22{,}300}{8.3144T}\right)$	49
$k_{t,0}$(BuA) (dm^3 mol^{-1} s^{-1})	$4000k_p$	50, 51
$k_{t,0}$(MMA) (dm^3 mol^{-1} s^{-1})	$27333k_p$	50
k_t^p	$k_{t,0}^p[a_1\varphi_p^p + b_1(\varphi_p^p)^2]$	Assumed
k_{tr}(BuA) (dm^3 mol^{-1} s^{-1})	$7.77 \times 10^{-5}\ k_p$	52
k_{tr}(MMA) (dm^3 mol^{-1} s^{-1})	$1.81 \times 10^{-5}\ k_p$	53
$[M_{\text{BuA}}]_{aq,sat}$ (mol dm^{-3})	0.064	1
$[M_{\text{BuA}}]_{p,sat}$ (mol dm^{-3})	5	54
$[M_{\text{MMA}}]_{aq,sat}$ (mol dm^{-3})	0.15	55
$[M_{\text{MMA}}]_{p,sat}$ (mol dm^{-3})	6.6	55
$r_{\text{BuA–MMA}}$	0.315	48
$r_{\text{MMA–BuA}}$	0.264	48
z	5	1

and that massive particle nucleation and coagulation may take place during the first moments of the polymerization.

A second polymerization run was conducted at similar operation conditions of the previous one, but this time with the addition of an electrolyte solution (4.4 g dm^{-3} of NaCl in the mixture) to increase the ionic strength of the reaction medium. As might be expected, the final number of polymer particles was much lower than that in the previous run (see Figure 4) because of coagulation between polymer particles throughout the polymerization process. This fact can be observed directly from experimental *Np* data. Figure 4 illustrates profiles 1 and 2 for the second run as defined previously. If the "experimental" profile (profile 1) is used in the kinetic model, the simulated conversion is significantly underestimated compared with the experimental conversion data. To properly describe the observed experimental monomer conversion, the *Np* profile 2 calculated by PBE with the kinetic model should be used. According to the results shown in Figure 4, the shape of the resulting *Np* profile 2 indicates that a large number of moderately short-lived particles are once again formed and then coagulate until an acceptable level of stabilization has been attained.

Concerning the nucleation behavior, it should be emphasized that some differences can be observed in the presence of electrolytes: (1) a lower number of particles are formed, resulting in large particles; (2) lower reaction rates are observed, resulting in a slower nucleation step; (3) more significant underestimation of monomer conversion is observed when the "experimental" *Np* profile is fed into the kinetic model, meaning that the kinetic model fed with the slower "experimental" *Np* profile provides poorer predictions of monomer conversion than in the case of faster reactions. Therefore, one can eliminate the idea that the kinetic model proposed here and validated for semibatch processes is unable to describe the batch processes, given that batch processes are normally faster than semibatch processes. All these points suggest that the kinetic model should not be blamed for the poor predictions obtained when the "experimental" *Np* profiles are used, which also give coherency of the results obtained in the simulations.

Results presented here are also corroborated by the independent calorimetric studies on the copolymerization of styrene and butyl acrylate reported by Othman et al.[44] Although the chemical composition of this system is not the same as that used in the model validations shown here, it nevertheless allows us to see the discrepancy between on-line and off-line measurements. As shown in Figure 5, high polymerization rates attributed to unstable renucleation were identified by the authors using a calorimetric strategy. It can be seen from this figure that, although the injection of monomer, initiator, and surfactant at 50 min provoked (as expected) a renucleation of particles, the rate of generation of heat resulting from polymerization increased more than one would expect from the increase in *Np*. The off-line values of *Np* show an increase of a factor of 3–3.5 after the shot injection. However, the rate of heat generation increases by a factor of 6. Because this quantity is directly proportional to the rate of reaction, and the rate is directly proportional to *Np*, these results suggest that a large number of very small polymer particles that could not be measured by available light-scattering techniques were formed in the reactor. Thus the shape of the *Np* profile obtained in the simulations seems to be realistic and merits additional investigation for a broader range of conditions and monomer systems.

Conclusions

In the current work, a mathematical framework that allows us to provide a quantitative description of the nucleation stage during batch emulsion polymerization processes was presented. Thus the thrust of this work was not to develop a "new" model for particle nucleation, but rather to show that we can to quantify it ab initio, using known models and experimental techniques. This allows one to quantify the differences between what is measured off-line by light scattering, and what is really occurring in the reactor. Each phenomenon involved in the emulsion polymerization process (coagulation, stabilization, monomer partitioning, and kinetics) was studied separately. These phenomena were successfully described independently of each other, both experimentally and theoretically, and then incorporated into a general mathematical framework in the form of a population balance equation.

The model provided *Np* estimates that are quite different from those generally reported in the literature for emulsion polymerizations, where most groups seem to rely entirely on off-line measurements of the number of particles to estimate the reaction parameters. For example, many models of the average number of radicals per particle developed for emulsion

Table 3. Parameter Values Used in the Nucleation Model

Parameter	Value	Reference
$a_{s,TA}$ (Å^2 molecule^{-1})	60	Experimental, 32
CMC_{TA} (g dm^{-3})	0.24	Experimental, 32
f_{mic}	0.6×10^{-4}	Estimated
r_{mic} (nm)	2.6	32

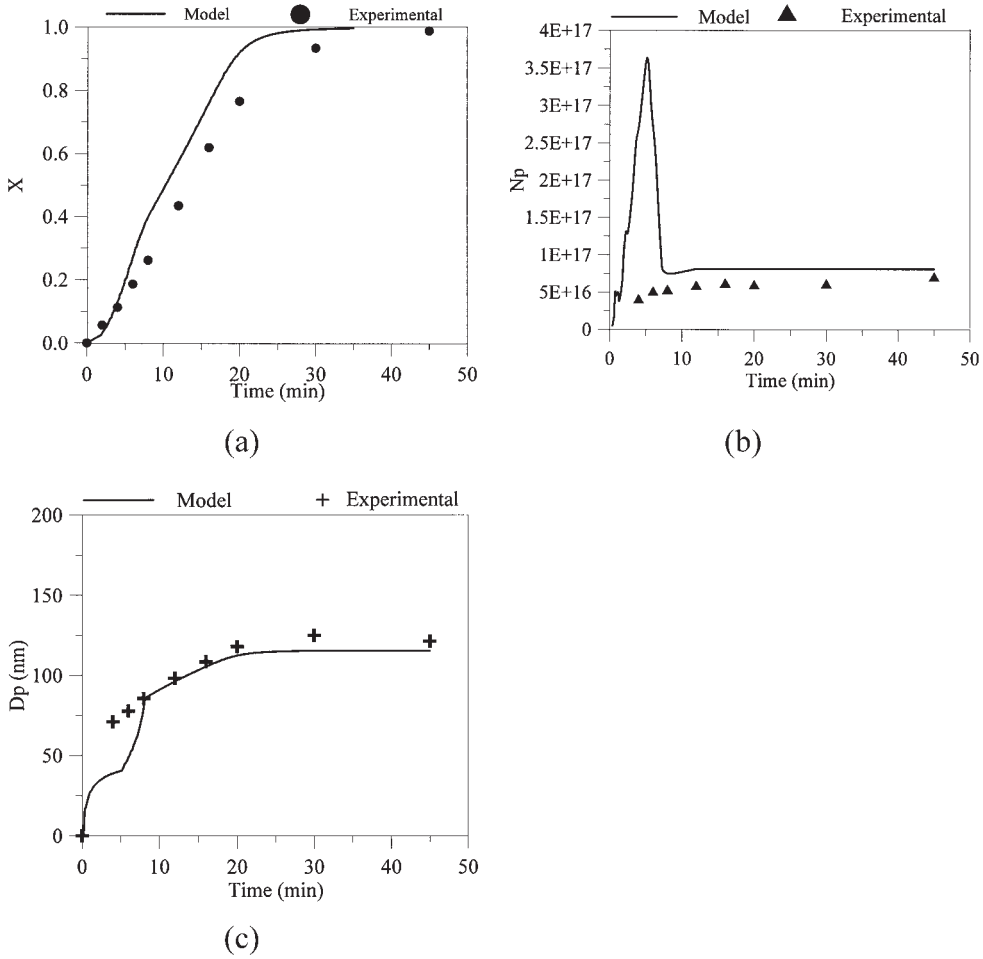

Figure 2. (A) Evolution of monomer conversion for the batch run. (B) Evolution of *Np* for the batch run. (C) Evolution of *Dp* for the batch run.

polymerization use off-line particle size measurements to back-calculate $\bar{n}$ from *Np*, and this can clearly lead to errors of interpretation.

Some additional points should be emphasized here: (1) there is one—and only one—adjustable parameter in the coagulation model, which is the Hamaker constant; (2) the kinetics of

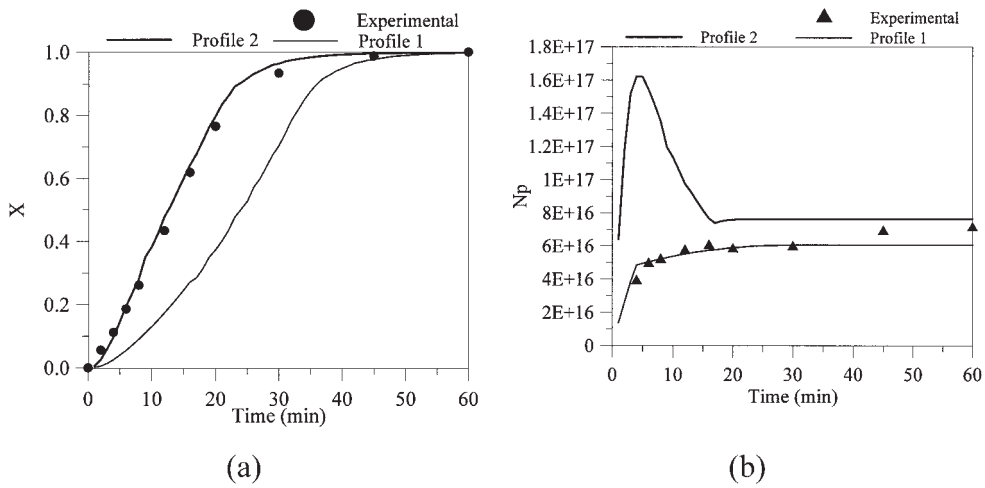

Figure 3. (A) Experimental and simulated monomer conversion for two different *Np* profiles for the batch run. (B) Experimental and assumed *Np* profiles for the batch run.

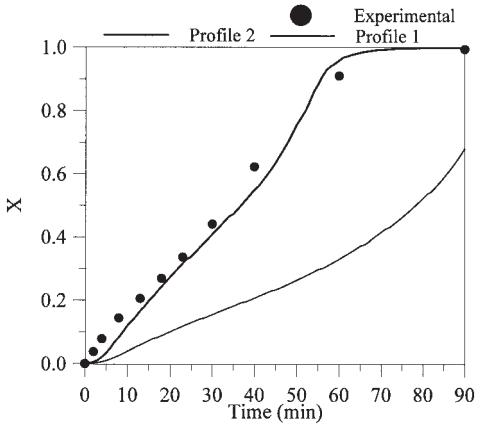

Figure 4. Experimental and simulated monomer conversion for two different *Np* profiles for the batch run with the electrolyte solution.

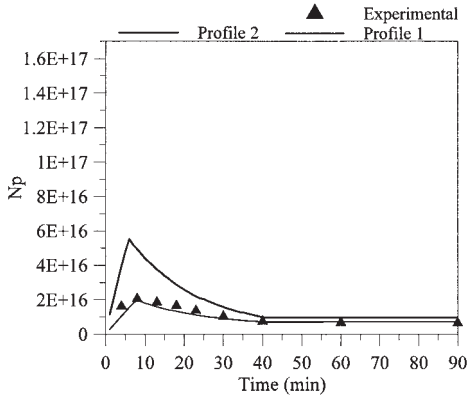

Figure 6. Experimental and assumed *Np* profiles for the batch run with the electrolyte solution.

coagulation have been validated in the absence of reaction; and (3) that the kinetics of polymerization has been validated in the absence of coagulation. It would be a very fortunate coincidence that having done this, the model predicts the value of *Np* as well as is shown in Figures 2b and 6. In fact, none of the previously published PBE approaches attempted to do this. Thus there are no hidden factors in the approach presented here, which gives us interesting insight into the evolution of the PSD during dynamic phases of the reaction.

This quantitative approach to modeling nucleation is quite useful for calculating a number of important quantities in addition to the kinetic parameters. For instance, Schneider et al.[45] reported difficulties in controlling a second population of particles in bimodal latices when this population was nucleated by shot injections of monomer. Their results showed that when one attempted to create a population of small particles by a route similar to that shown in Figure 5, one often encounters problems of latex destabilization, which the authors attributed to a redistribution of the available surfactant in the reactor resulting from an uncontrolled renucleation of small particles. Thus, if correctly adapted to this type of system, the approach presented here would allow one to exert a stricter control over complex PSDs.

Acknowledgments

The authors are grateful to Atofina (now Arkema) and Crayvalley for financial support of this work.

Notation

a_1 = gel effect constant
$a_{s,TA}$ = minimum area occupied by single surfactant molecule on particle surface, Å^2 molecule^{-1}
b_1 = gel effect constant
CMC_{TA} = micellar critical concentration of surfactant, g dm^{-3}
D_{aq} = diffusion coefficient for monomer in water, dm^2 s^{-1}
Dp = diameter of polymer particles, nm
f_{mic} = efficiency of the radical entry into micelles
$f(m, t)$ = particle fraction of particles of mass m at time t

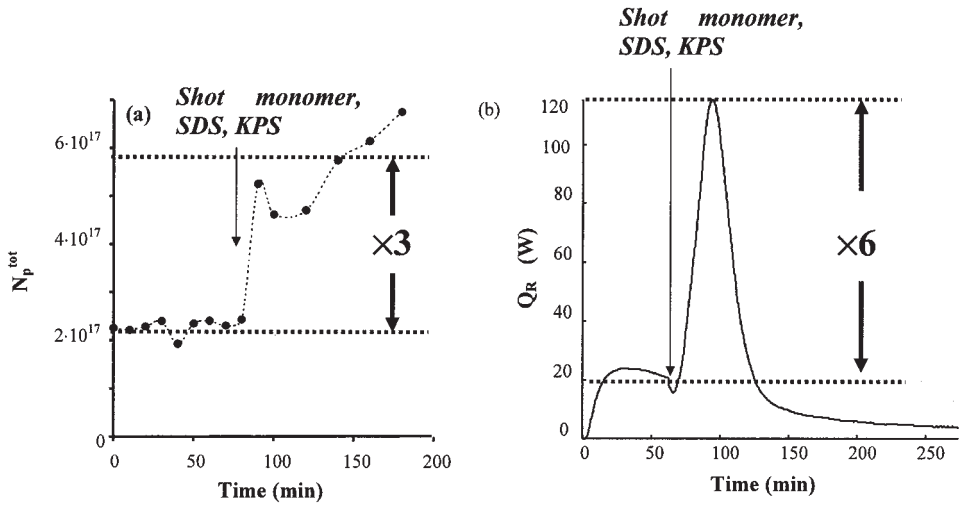

Figure 5. Evolution of the total number of particles in a seeded, semibatch copolymerization of styrene and butyl acrylate (left) and the rate of generation of heat by the reaction (right).

Reaction conditions: 90 g polystyrene seed, 143 g butyl acrylate (BA), 116 g styrene (Sty), 9 g sodium dodecyl sulfate (SDS), 1.2 g potassium persulfate (KPS), 2630 g water, and a temperature of 60°C. The shot at 50 min contained 149 g BA, 162 g Sty, 1.5 g KPS, 24 g SDS, and 30 g water. Further details available in Othman et al.[44]

j_{crit} = critical degree of polymerization for particle formation
k_B = Boltzmann constant, J K^{-1}
k_{mic} = coefficient rate for radical entry into micelles, dm^3 mol^{-1} s^{-1}
k_p = propagation rate coefficient, dm^3 mol^{-1} s^{-1}
$k_{t,0}$ = termination rate coefficient at zero polymer content, dm^3 mol^{-1} s^{-1}
k_t^p = termination rate coefficient, dm^3 mol^{-1} s^{-1}
k_{tr} = radical transfer rate coefficient, dm^3 mol^{-1} s^{-1}
$[M]_{aq,sat}$ = saturation monomer concentration in the aqueous phase, mol dm^{-3}
$[M]_{p,sat}$ = saturation monomer concentration in the polymer particles, mol dm^{-3}
Np = number of polymer particles
N_{mic} = micelle concentration, dm^{-3}
$NucHo$ = homogeneous nucleation rate, dm^{-3} s^{-1}
$NucMi$ = micellar nucleation rate, dm^{-3} s^{-1}
r_{A-B} = reactivity ratio for polymerization of radical polymer chain of type A with monomer of type B
r_{mic} = micelle ratio, nm
T = temperature, K
W_{ij} = Fuch's stability ratio
z = critical degree of polymerization for radical entry
β_{ij} = coagulation rate between ith- and jth-type particles, m^3 s^{-1}
η = latex viscosity, kg m^{-1} s^{-1}

Literature Cited

1. Gilbert RG. *Emulsion Polymerization: A Mechanistic Approach*. London: Academic Press; 1995.
2. El-Aasser MS, Sudol ED. Features of emulsion polymerization. In: Lovell PA, El-Aasser MS, eds. *Emulsion Polymerization and Emulsion Polymers*. New York, NY: Wiley; 1997:37-58.
3. Gilbert RG, Morrison BR, Napper DH. The status of nucleation models in emulsion polymerization. *Polym Mater Sci Eng*. 1991;64: 308-309.
4. Santos AF, Lima EL, Pinto JC, Graillat C, McKenna TF. On-line monitoring of the evolution of the number of particles in emulsion polymerization by conductivity measurements. I. Model formulation. *J Appl Polym Sci*. 2003;90:1213-1226.
5. Novak RW. Mechanism of acrylic emulsion polymerizations. *Adv Org Coat Sci Technol Ser*. 1988;10:54-57.
6. Feeney PJ, Napper DH, Gilbert RG. Coagulative nucleation and particle size distributions in emulsion polymerization. *Macromolecules*. 1984;17:2520-2529.
7. Morrison BR, Maxwell IA, Gilbert RG, Napper DH. *Testing Nucleation Models for Emulsion–Polymerization Systems*. American Chemical Society Symposium Series 492. New York, NY: ACS; 1992:38-44.
8. Lichti G, Gilbert RG, Napper DH. Particle nucleation in emulsion polymerization. II. Nucleation in emulsifier-free-systems investigated by seed polymerization. *J Polym Sci Part A: Polym Chem*. 1983;21: 269-291.
9. Vanderhoff JW. The formation of coagulum in emulsion polymerization. In: Bassett DR, Hamielec AE, eds. *Emulsion Polymers and Emulsion Polymerization*. Washington, DC: ACS; 1981:199-208.
10. Lowry V, El-Aasser MS, Vanderhoff JW, Klein A. Mechanical coagulation in emulsion polymerizations. *J Appl Polym Sci*. 1984;29:3925-3935.
11. Matejícek A, Pivonková A, Kaška J, Ditl P, Formánek L. Influence of agitation on the creation of coagulum during the emulsion polymerization of the system styrene–butylacrylate–acrylic acid. *J Appl Polym Sci*. 1988;35:583-591.
12. Chern CS, Kuo YN. Shear-induced coagulation kinetics of semibatch seeded emulsion polymerization. *Chem Eng Sci*. 1996;51:1079-1087.
13. Lowry V, El-Aasser MS, Vanderhoff JW, Klein A, Silebi CA. Kinetics of agitation-induced coagulation of high-solid latexes. *J Colloid Interface Sci*. 1986;112:521-529.
14. Harkins WD. A general theory of the reaction loci in emulsion polymerization. *J Chem Phys*. 1945;13:381-382.
15. Harkins WD. A general theory of the reaction loci in emulsion polymerization. II. *J Chem Phys*. 1946;14:47-48.
16. Harkins WD. A general theory of the reaction loci in emulsion polymerization. III. *J Am Chem Soc*. 1947;69:1428-1429.
17. Fitch RM. Homogeneous nucleation of polymer colloids. *Br Polym J*. 1973;5:467-483.
18. Hansen FK, Ugelstadt J. Particle nucleation in emulsion polymerization. I. A theory for homogeneous nucleation. *J Polym Sci Polym Chem Ed*. 1978;16:1953-1979.
19. Lichti G; Gilbert RG, Napper DH. The mechanisms of latex particle formation and growth in the emulsion polymerization of styrene using the surfactant sodium dodecyl sulphate. *J Polym Sci Polym Chem Ed*. 1983;21:269-291.
20. Ugelstad J, El-Aasser MS, Vanderhoff J. Emulsion polymerization. Initiation of polymerization in monomer droplets. *J Polym Sci Lett*. 1973;11:503-513.
21. Ugelstad J, Hansen FK, Lange S. Emulsion polymerization of styrene with sodium hexadecyl sulfate–hexadecanol mixtures as emulsifiers. Initiation in monomer droplets. *Makromol Chem*. 1974;175:507-521.
22. Novak RW. Mechanism of acrylic emulsion polymerizations. *Adv Org Coat Sci Technol Ser*. 1988;10:54-57.
23. Forcolin S, Marconi AM, Ghielmi A, Butté A, Storti G, Morbidelli M. Coagulation phenomena in emulsion polymerization of vinyl chloride. *Plast Rubber Compos*. 1999;28:109-115.
24. Unzueta E, Forcada J. Modeling the effect of mixed emulsifier systems in emulsion copolymerization. *J Appl Polym Sci*. 1997;66:445-458.
25. Coen EM, Peach S, Morrison BR, Gilbert RG. First-principles calculation of particle formation in emulsion polymerization: Pseudo-bulk systems. *Polymer*. 2004;45:3595-3608.
26. Gao J, Penlidis A. Mathematical modeling and computer simulator/database for emulsion polymerization. *Prog Polym Sci*. 2002;27:403-535.
27. Coen EM, Gilbert RG, Morrison BR, Leube H, Peach S. Modelling particle size distribution and secondary particle formation in emulsion polymerization. *Polymer*. 1998;39:7099-7112.
28. Forcada J, Asua JM. Modeling of unseeded emulsion copolymerization of styrene and methyl methacrylate. *J Polym Sci Part A: Polym Chem*. 1990;28:987-1009.
29. Saldivar E, Dafniotis P, Ray WH. Mathematical modeling of emulsion copolymerization reactors. I. Model formulation and application to reactors operating with micellar nucleation. *J Macromol Sci Rev Macromol Chem Phys*. 1998;C38:207-325.
30. Elizalde O, Leal GP, Leiza JR. Particle size measurements of polymeric dispersions. *Part Part Syst Char*. 2000;17:236-243.
31. Schneider M, McKenna TF. Comparative study of methods for the measurement of particle size and size distribution of polymeric emulsions. *Part Part Syst Char*. 2002;19:28-37.
32. Fortuny M. *Modélisation de Procédés pour la Synthèse de Latex Multipopulés* (in French). PhD Thesis. Lyon, France: Université Claude Bernard Lyon I; 2002.
33. Fortuny M, Graillat C, McKenna TF. Coagulation of polymer particles stabilized electrosterically. *Ind Eng Chem Res*. 2004;43:7210-7219.
34. Fortuny M, Graillat C, McKenna TF. A new technique for the experimental measurement of monomer partition coefficients. *Macromol Chem Phys*. 2004;205:1309-1319.
35. Araújo PHH. *Distribuição de Tamanhos de Partícula em Sistemas Heterogêneos de Polimerização* (in Portuguese). PhD Thesis. Rio de Janeiro, Brazil: Universidade Federal do Rio de Janeiro; 1999.
36. Araújo PHH, de La Cal JC, Asua JM, Pinto JC. Modeling particle size distribution (PSD) in emulsion copolymerization reactions in a continuous loop reactor. *Macromol Theor Simul*. 2001;10:769-779.
37. Ugelstad J, Mork PC, Aasen JO. Kinetics of emulsion polymerization. *J Polym Sci Part A-1*. 1967;5:2281-2288.
38. Maxwell IA, Kurja J, Van Doremaele GHL, German AL. Partial swelling of latex particles with monomers. *Makromol Chem*. 1992; 193:2049-2063.
39. Maxwell IA, Noël LFJ, Schoonbrood HAS, German AL. Thermodynamics of swelling of latex particles with two monomers: A sensitivity analysis. *Makromol Chem Theor Simul*. 1993;2:269-274.
40. Verwey EJW, Overbeek JThG. *Theory of the Stability of Lyophobic Colloids*. Mineola, NY: Dover Publications; 1999.
41. Deryaguin BV, Landau, LD. In: Lyklema, J, ed. *Fundamentals of Interface and Colloid Science. Vol. I. Solid–Liquid Interfaces*. London: Academic Press; 1995.
42. Hidalgo-Álvarez R, Martín A, Fernández A, Bastos D, Martínez F, de las Nieves FJ. Electrokinetic properties, colloidal stability and aggregation kinetics of polymer colloids. *Adv Colloid Interface Sci*. 1996; 67:1-118.

43. Petzold LR. A differential algebraic system solver. Report #SAND82-8637. Albuquerque, NM: Sandia National Laboratories; 1982.
44. Othman N, Santos AM, Fevotte G, McKenna TF. Monitoring of emulsion polymerisations: A study of reaction kinetics in the presence of secondary nucleation. *Can J Chem Eng*. 2002;80:88-104.
45. Schneider M, Graillat C, Guyot A, McKenna TF. High solids content emulsions. III. Synthesis of concentrated latices via classic emulsion polymerization. *J Appl Polym Sci*. 2002;84:1916-1934.
46. Bird RB, Stewart WE, Lightfoot EN. *Transport Phenomena*. New York, NY: Wiley; 1960.
47. Beuermann S, Paquet DA, McMinn JH, Hutchinson RA. Determination of free-radical propagation rate coefficients of butyl, 2-ethylhexyl and dodecyl acrylates by pulsed-laser polymerization. *Macromolecules*. 1996;29:4206-4215.
48. Aerdts AM, German AL. Determination of the reactivity ratios, sequence distribution and stereoregularity of butyl acrylate–methyl methacrylate copolymers by means of proton and carbon-13 NMR. *Magn Reson Chem*. 1994;32:S80-S88.
49. Beuermann S, Buback M, Davis TP, Gilbert RG, Hutchinson RA, Olaj OF, Russell GT, Schweer J, Van Herk AM. Critically evaluated rate coefficients for free-radical polymerization, 2. Propagation rate coefficients for methyl methacrylate. *Macromol Chem Phys*. 1997;198:1545-1560.
50. Buback M, Kowollik C. Termination kinetics of methyl methacrylate free-radical polymerization studied by time-resolved pulsed laser experiments. *Macromolecules*. 1998;31:3211-3215.
51. Buback M, Degener B. Rate coefficients for free-radical polymerization of butyl acrylate to high conversion. *Makromol Chem*. 1993;194:2875-2883.
52. Maeder S, Gilbert RG. Measurement of transfer constant for butyl acrylate free-radical polymerization. *Macromolecules*. 1998;31:4410-4418.
53. Stickler M, Meyerhoff G. Die thermische polymerisation von methylmethacrylat, 1. Polymerisation in substanz. *Makromol Chem*. 1978;179:2729-2745.
54. Gardon JL. Emulsion polymerization. IV. Concentration of monomers in latex particles. *J Polym Sci Polym Chem Ed*. 1968;6:2859-2879.
55. Ballard MJ, Napper DH, Gilbert RG. Kinetics of emulsion polymerization of methyl methacrylate. *J Polym Sci Part A: Polym Chem*. 1984;22:3225-3253.
56. Storti G, Morbidelli M, Carra S. Detailed modeling of multicomponent emulsion polymerization systems. In: Provder T, ed. *Computer Applications in Applied Polymer Science II: Automation, Modeling and Simulation*. American Chemical Society Symposium Series 404. New York, NY: ACS; 1989:379-402.
57. Storti G, Carra S, Morbidelli M, Vita G. Kinetics of multimonomer emulsion polymerization. The pseudo-homopolymerization approach. *J Appl Polym Sci*. 1989;37:2443-2467.
58. Sayer C, Arzamendi G, Asua JM, Lima EL, Pinto JC. Dynamic optimization of semicontinous emulsion copolymerization reactions: Composition and molecular weight distribution. *Comput Chem Eng*. 2001;25:839-849.
59. Asua JM, Sudol ED, El-Aasser MS. Radical desorption in emulsion polymerization. *J Polym Sci Part A: Polym Chem*. 1989;27:3903-3913.

Appendix: Kinetic Model

The kinetic model used here is based on the pseudo-bulk approximation, and neglects radical compartmentalization in the particles. The following hypotheses were invoked:

- Isothermal reactions.
- Steady-state hypothesis for the radicals in the particle and aqueous phases.
- Reactivity of the growing radicals depends only on the ultimate radical and is independent of chain length.
- Propagation and transfer constants are identical in the particle and aqueous phases.

In the following paragraphs, we will develop the expressions for the batch reaction and the radical balances. The semibatch expressions can easily derived from these balances simply by adding the inlet flow rates. The evolution of the molar concentration of monomers in the reactor are given by the following expressions:

$$V_R \frac{d[M_A]}{dt} = -\frac{\bar{n}Np[M_A]_p}{N_A}\left(k^p_{pAA}P^p_A + k^p_{pBA}P^p_B\right) - [R_{TOT}]_{aq}[M_A]_{aq}V^{aq}\left(k^{aq}_{pAA}P^{aq}_A + k^{aq}_{pBA}P^{aq}_B\right) \quad \text{(A1)}$$

$$V_R \frac{d[M_B]}{dt} = \frac{\bar{n}Np[M_B]_p}{N_A}\left(k^p_{pBB}P^p_B + k^p_{pAB}P^p_A\right) - [R_{TOT}]_{aq}[M_B]_{aq}V^{aq}\left(k^{aq}_{pBB}P^{aq}_B + k^{aq}_{pAB}P^{aq}_A\right) \quad \text{(A2)}$$

The probabilities P_A and P_B in the particle and aqueous phases (superscripts p and aq, respectively) are calculated by assuming that the radical concentrations are at pseudo-steady state and are given by

$$P^p_A = \frac{[R_A]_p}{[R_A]_p + [R_B]_p} = \frac{k^p_{pBA}[M_A]_p}{k^p_{pBA}[M_A]_p + k^p_{pAB}[M_B]_p} \qquad P^p_A = 1 - P^p_B \quad \text{(A3)}$$

$$P^{aq}_A = \frac{[R_A]_{aq}}{[R_A]_{aq} + [R_B]_{aq}} = \frac{k^{aq}_{pBA}[M_A]_{aq}}{k^{aq}_{pBA}[M_A]_{aq} + k^{aq}_{pAB}[M_B]_{aq}} \qquad P^{aq}_A = 1 - P^{aq}_B \quad \text{(A4)}$$

The initiator balance is written as

$$V_R \frac{d[I]}{dt} = -k_{dec}[I]V^{aq} \quad \text{(A5)}$$

The surfactant is partitioned between the particles, micelles and aqueous phases, so the total mass of surfactant in the reactor obeys

$$V_R[TA_a] = V^{aq}[TA_a]_{aq} + S_p[TA_a]_p + T_{mic}N_{mic} \quad \text{(A6)}$$

where N_{mic} is the number of micelles and T_{mic} is the mass of surfactant per micelle, calculated from

$$T_{mic} = \frac{N_{aq}MM(TA)}{N_A} \quad \text{(A7)}$$

where N_{ag} is the aggregation number of the micelles, and $MM(TA)$ is the molecular weight of the surfactant. If micelles are present, it is assumed that the particles are essentially totally covered with surfactant. Thus the amount of surfactant on the particles is

$$[TA_a]_p = \frac{MM(TA_a)}{a_{s,TAa}N_A} \quad \text{(A8)}$$

In the absence of any micelles, the surfactant is situated preferentially on the surface of the particles.

If present, the number of micelles is calculated from (and is obviously set to zero if the result is negative):

$$N_{mic} = \frac{1}{T_{mic}} (V_R[TA] - V^{aq}[TA]_{aq} - S_p[TA]_p) \tag{A9}$$

The reaction volume is calculated from

$$\begin{aligned}\frac{dV_R}{dt} = &- \frac{\bar{n}Np[M_A]_p}{N_A} (k^p_{pAA}P^p_A + k^p_{pBA}P^p_B)\left(\frac{1}{d_{M_A}} - \frac{1}{d_{Pol_A}}\right) \\ &- \frac{\bar{n}Np[M_B]_p}{N_A} (k^p_{pBB}P^p_B + k^p_{pAB}P^p_A)\left(\frac{1}{d_{M_B}} - \frac{1}{d_{Pol_B}}\right) \\ &- [R_{TOT}]_{aq}[M_A]_{aq}V^{aq}(k^{aq}_{pAA}P^{aq}_A + k^{aq}_{pBA}P^{aq}_B)\left(\frac{1}{d_{M_A}} - \frac{1}{d_{Pol_A}}\right) \\ &- [R_{TOT}]_{aq}[M_B]_{aq}V^{aq}(k^{aq}_{pBB}P^{aq}_B + k^{aq}_{pAB}P^{aq}_A)\left(\frac{1}{d_{M_B}} - \frac{1}{d_{Pol_B}}\right)\end{aligned} \tag{A10}$$

The radical balance in the aqueous phase depends on the rate of entry of radicals of length $\geq z_{crit}$ into the particles, the rate of precipitation of oligoradicals of length $\geq j_{crit}$, the rate of desportion of radicals from the particles and the rate of generation of polymerizable radicals in the water phase. The total radical concentration in the water phase is given by the following expression where k is the length of a water-soluble oligoradical.

$$[R_{TOT}]_{aq} = \sum_{i=1}^{j_{crit}-1} [R_k]_{aq} \tag{A11}$$

The concentration of radicals of length one is given by

$$[R_1]_{aq} = \frac{2fk_{dec}[I] + \dfrac{\bar{k}_d\bar{n}}{N_A V^{aq}} Np}{(k^{aq}_{pAA}P^{aq}_A + k^{aq}_{pBA}P^{aq}_B)[M_A]_{aq} + (k^{aq}_{pBB}P^{aq}_B + k^{aq}_{pAB}P^{aq}_A)[M_B]_{aq} + \bar{k}^{aq}_t[R_{TOT}]_{aq}} \tag{A12}$$

where $\bar{k}_d$ and $\bar{k}^{aq}_t$ are the average constants for desorption and termination of radicals, respectively; and f is the initiator efficiency. The pseudo-homopolymer rate constant is calculated as suggested elsewhere in the literature[56,57]:

$$\bar{k}^{aq}_t = k^{aq}_{tAA}(P^{aq}_A)^2 + 2k^{aq}_{tAB}P^{aq}_A P^{aq}_B + k^{aq}_{tBB}(P^{aq}_B)^2 \tag{A13}$$

The concentration of radicals of length $k = 2 \cdots z_{\text{crit}} - 1$ is given by the following series of equations:

$$[R_k]_{aq} = \frac{\varepsilon_1[R_{k-1}]_{aq}}{\varepsilon_2} \tag{A14}$$

$$\varepsilon_1 = (k^{aq}_{pAA}P^{aq}_A + k^{aq}_{pBA}P^{aq}_B)[M_A]_{aq} + (k^{aq}_{pBB}P^{aq}_B + k^{aq}_{pAB}P^{aq}_A)[M_B]_{aq} \tag{A15}$$

$$\varepsilon_2 = (k^{aq}_{pAA}P^{aq}_A + k^{aq}_{pBA}P^{aq}_B)[M_A]_{aq} + (k^{aq}_{pBB}P^{aq}_B + k^{aq}_{pAB}P^{aq}_A)[M_B]_{aq} + \bar{k}^{aq}_t[R_{TOT}]_{aq} \tag{A16}$$

So that

$$[R_k]_{aq} = [R_1]_{aq}\left(\frac{\varepsilon_1}{\varepsilon_2}\right)^{k-1} \tag{A17}$$

The concentration of radicals with a degree of polymerization between z_{crit} and $j_{crit} - 1$ can be calculated as follows:

$$[R_k]_{aq} = \frac{\varepsilon_1[R_{k-1}]_{aq}}{\varepsilon_2 + \dfrac{(k_{abs}Np + k_{amic}N_{mic})}{V_R N_A}} \tag{A18}$$

where k_{abs} and k_{amic} are the constants of radical entry into the particles and the micelles, respectively:

$$\varepsilon_3 = \frac{(k_{abs} + k_{amic}N_{mic})}{V_R N_A} \tag{A19}$$

$$[R_k]_{aq} = [R_1]_{aq}\left(\frac{\varepsilon_1}{\varepsilon_2}\right)^{z_{crit}-2}\left(\frac{\varepsilon_1}{\varepsilon_2 + \varepsilon_3}\right)^{k-z_{crit}+1} \tag{A20}$$

The total radical concentration in the aqueous phase, $[R_{TOT}]_{aq}$, and the total radical concentration capable of entering into particles and micelles are given by

$$[R_{TOT}]_{aq} = [R_1]_{aq}\left[1 + \sum_{2}^{z_{crit}-1}\left(\frac{\varepsilon_1}{\varepsilon_2}\right)^{k-2} + \left(\frac{\varepsilon_1}{\varepsilon_2}\right)^{z_{crit}-2}\sum_{z_{crit}}^{j_{crit}-1}\left(\frac{\varepsilon_1}{\varepsilon_2 + \varepsilon_3}\right)^{k-z_{crit}+1}\right] \tag{A21}$$

$$[R_{ent}]_{aq} = [R_1]_{aq}\left(\frac{\varepsilon_1}{\varepsilon_2}\right)^{z_{crit}-2}\sum_{z_{crit}}^{j_{crit}-1}\left(\frac{\varepsilon_1}{\varepsilon_2 + \varepsilon_3}\right)^{k-z_{crit}+1} \tag{A22}$$

The different entry constants are given by[26]

$$k_{abs} = 4\pi D_{aq} r_{pg} N_A f_{abs} \tag{A23}$$

$$k_{amic} = 4\pi D_{aq} r_{mic} N_A f_{amic} \tag{A24}$$

where the constants f_{abs} and f_{amic} are the efficiencies of radical absorption into the particles and micelles, respectively; r_{pg} and r_{mic} the radii of a swollen particle and a micelle, respectively; and D_{aq} is the diffusion coefficient of the radicals in the aqueous phase.

In a pseudo-bulk system $\bar{n}$ is found according to the derivation presented in the literature[37]:

$$\bar{n} = \frac{1}{2}\cfrac{h^2/4}{m + 0 + \cfrac{h^2/4}{m + 1 + \cfrac{h^2/4}{m + 2 + \cdots}}} \tag{A25}$$

$$h = \left(\frac{8\bar{\rho}}{\bar{k}_t^p}\right)^{0.5} \qquad \text{where } \bar{\rho} = k_{abs} N_A \nu_p [R_{ent}]_{aq} \tag{A26}$$

$$m = \frac{k_{des}}{\bar{k}_t^p} \qquad \text{where } k_{des} = \bar{k}_d N_A \nu_p \tag{A27}$$

where ν_p is the volume of a particle and $\bar{k}_t^p$ is the termination rate constant in the particles. This latter constant is once again calculated using the pseudo-homopolymerization method proposed by Storti et al.,[56,57] and a gel effect correction (fitted from experimental data) of the following form[58] is also used:

$$\bar{k}_{t0}^p = k_{t0,AA}^p (P_A^p)^2 + 2k_{t0,AB}^p P_A^p P_B^p + k_{t0,BB}^p (P_B^p)^2 \tag{A28}$$

$$\bar{k}_t^p = k_{t0}^p [a_1 \phi_p^p + b_1 (\phi_p^p)^2] \tag{A29}$$

with $a_1 = -4.03$ and $b_1 = -0.66$.[32]

The average value of the overall desorption constant is calculated from the individual values as follows[56,57]:

$$\bar{k}_d = k_{d,M_A} + k_{d,M_B} \tag{A30}$$

The individual desorption coefficients are calculated by[59]

$$k_{d,i} = (k_{tr,M_A} P_A^p + k_{tr,M_{Bi}} P_B^p)[i]_p \frac{k_{0,i}}{k_{0,i}\beta_i + k_{piA}^p [M_A]_p + k_{piB}^p [M_B]_p} \tag{A31}$$

where β_i is the probability that a monomeric radical of type i will react in the aqueous phase by propagation or by termination:

$$\beta_i = \frac{(k_{piA}^{aq}[M_A]_{aq} + k_{piB}^{aq}[M_B]_{aq}) + (k_{t,M_{Ai}}^{aq} P_A^{aq} + k_{t,M_{Bi}}^{aq} P_B^{aq})[R_{TOT}]_{aq}}{k_{abs}\dfrac{Np}{V^{aq} N_A} + (k_{piA}^{aq}[M_A]_{aq} + k_{piB}^{aq}[M_B]_{aq}) + (k_{t,M_{Ai}}^{aq} P_A^{aq} + k_{t,M_{Bi}}^{aq} P_B^{aq})[R_{TOT}]_{aq}} \tag{A32}$$

and k_{0i} is the rate of diffusion of monomeric radicals of type i toward the aqueous phase in the absence of other types of resistance:

$$k_{0i} = \frac{12\dfrac{D_{aq,i}}{m_{di} d_p^2}}{1 + 2\dfrac{D_{aq,i}}{m_{di} D_{p,i}}} \tag{A33}$$

where $D_{aq,i}$ and $D_{p,i}$ are the diffusion coefficients of a monomeric radical of type i in the aqueous and particle phases, respectively; m_{di} is the partition coefficient of radicals between the particles and water; and d_p is the particle diameter. It is supposed that monomeric radicals partition in the same manner as the monomer molecules. The above equations are used to calculate $[R_{TOT}]_{aq}$ and $\bar{n}$ as follows:

(1) Provide initial guesses for $[R_{TOT}]_{aq}$ and $\bar{n}$.
(2) Calculate $[R_{ent}]_{aq}$ using Eqs. A21 and A22.
(3) $\bar{n}$ is calculated using Eq. A25.
(4) $[R_1]_{aq}$ is then calculated from Eq. A12.
(5) A new value of $[R_{TOT}]_{aq}$ is then calculated and the process continues until the value of this parameter converges.

Particles can be formed by entry of radicals into the micelles, or by precipitation of particles from the aqueous phase (homogeneous nucleation). Thus the rate of change of the number of particles of a given size will be the sum of the rates of micellar and homogeneous nucleation less the rate of disappearance by coagulation. The rates of nucleation are given by Eqs. 1 and 2 in the main body of the text.

Because the above equations are valid for only one size of particle, they are incorporated into a population balance to allow us to follow the evolution of the particle size distribution as described in the main body of the text.

Manuscript received July 12, 2004, and revision received Jan. 13, 2005.